



## Air-sea interaction over the Atlantic warm pool in the NCEP CFS

Vasubandhu Misra,<sup>1,2</sup> Steven Chan,<sup>2</sup> Renguang Wu,<sup>3</sup> and E. Chassignet<sup>2</sup>

Received 16 April 2009; revised 23 May 2009; accepted 30 June 2009; published 1 August 2009.

[1] This study shows that the SST variations in the July–August–September (JAS) peak season of the Atlantic Warm Pool (AWP) are modulated by the air-sea fluxes. This feature is captured in the correlations between the rainfall and SST, and rainfall and SST tendency in the multi-decadal integration of the National Centers for Environmental Prediction (NCEP) Climate Forecast System (CFS). Likewise, similar correlations are obtained from the NCEP CFS integration when latent heat flux is correlated with SST and SST tendency. However, when the same Atmospheric General Circulation Model as in the NCEP CFS (also called Global Forecast System [GFS]) is forced with observed SST, then the influence of air-sea fluxes on SST is lost. Further analysis of observed air-sea fluxes over the AWP region indicates that surface evaporation is weakly influenced by surface winds and air-sea humidity variations. But in the NCEP CFS and more so in the NCEP GFS, the latent heat flux, contrary to observations, is strongly modulated by the air-sea humidity variations. **Citation:** Misra, V., S. Chan, R. Wu, and E. Chassignet (2009), Air-sea interaction over the Atlantic warm pool in the NCEP CFS, *Geophys. Res. Lett.*, 36, L15702, doi:10.1029/2009GL038737.

### 1. Introduction

[2] The Atlantic Warm Pool (AWP) is a region within the Gulf of Mexico (GoM), the Caribbean Sea, and the western part of the tropical Atlantic Ocean with SST  $\geq 28.5^{\circ}\text{C}$ . It is part of the larger western hemisphere warm pool, which also includes parts of the tropical eastern Pacific Ocean [Wang and Enfield, 2001], and is considered a potential source of predictability for summer rainfall over the U.S., including the large-scale conditions that relate to Atlantic hurricane activity [Wang et al., 2006]. The AWP reaches its annual maximum areal extent during the July–August–September (JAS) season, when it is positively correlated with rainfall over the Caribbean, Mexico, Central America, and southeast Pacific, and negatively correlated with rainfall over the northwest U.S., U.S. Great Plains region, and eastern South America [Wang and Enfield, 2001, 2003; Wang et al., 2006, 2008a]. This modulation of boreal summer season rainfall over the Central U.S. is largely due to the influence of the anomalous AWP on the southerly Great Plains low level jet and hence the moisture transport in the region [Ruiz-Barradas

and Nigam, 2005; Wang et al., 2008a]. The AWP also appears to influence the vertical shear in the main development region of the tropical hurricanes in the Atlantic [Wang et al., 2008a]. Wang et al. [2008b] also indicate that AWP-induced atmospheric changes act as a conduit for the observed influence of the Atlantic multi-decadal oscillation on tropical cyclone activity.

[3] A disconcerting factor is that, in the majority of the global models that participated in the International Panel for Climate Change (IPCC) Assessment Report 4 (AR4), AWP cannot even be defined. The mean JAS SST bias in 8 of the IPCC AR4 models is shown in Figure S1 of the auxiliary material.<sup>4</sup> These models seem to suffer from a mean cold bias over the region. An intriguing feature of this warm pool is that the heaviest rainfall is not co-located over the region but in the neighboring continental regions. Furthermore, the interannual variability of the area of the AWP is largely independent of the El Niño–Southern Oscillation (ENSO) variation in the east Pacific, with nearly two thirds of the overall anomalous AWP events occurring independent of the ENSO events [Wang et al., 2006]. Therefore it is argued that the AWP variability may be a unique source of predictability of the boreal summer season rainfall. In this study, we present results from the National Centers for Environmental Prediction (NCEP) Climate Forecast System (CFS) [Saha et al., 2006], which is far more encouraging in its AWP simulation. The readers are, however, forewarned that unlike the IPCC class of models, the NCEP CFS is not a fully coupled climate system. Sea-ice is prescribed from observations in the NCEP CFS. So in some ways it may be argued that it is unfair to compare the IPCC class of models with NCEP CFS. The IPCC AR4 model bias is shown just to illustrate that the bias over the AWP region is grave in the current state of the art coupled climate models.

### 2. Experiment Design

[4] The coupled model results presented here are from a 32-year integration from one of the four ensemble members, made available on the NOAA web site (<http://cfs.ncep.noaa.gov>). This experiment is hereafter referred to as EXPT-C. The results of this study are nearly replicated in the other ensemble members (not shown), which suggest that the conclusion of this study on the NCEP CFS is robust. Similarly, the AGCM (NCEP Global Forecast System [GFS]) identical to that used in the EXPT-C experiment is integrated for 50 years from 1950–2000 with observed SST from the NOAA optimally interpolated version 2 following Reynolds et al. [2002]. This experiment hereafter is called EXPT-U. The focus of this study is on the JAS season,

<sup>1</sup>Department of Meteorology, Florida State University, Tallahassee, Florida, USA.

<sup>2</sup>Center for Ocean-Atmospheric Prediction Studies, Florida State University, Tallahassee, Florida, USA.

<sup>3</sup>Center for Ocean-Land-Atmosphere Studies, Calverton, Maryland, USA.

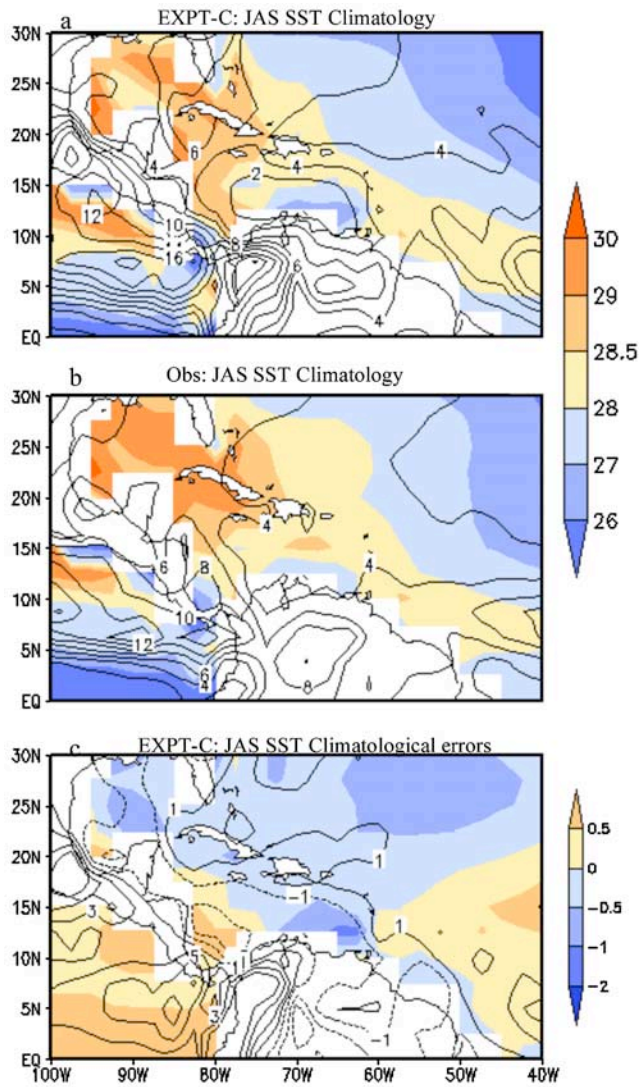


**Figure 1.** The climatological mean July–August–September (JAS) SST from (a) EXPT-C and (b) observations (ERSSTV2) [Reynolds *et al.*, 2002]. (c) Climatological JAS mean SST errors of EXPT-C. The corresponding climatological mean JAS rainfall (mm/day) is also overlaid as contours. The observed rainfall in Figures 1b and 1c is from Xie and Arkin [1997].

during which the AWP is at its annual maximum [Wang and Enfield, 2001].

### 3. Results

#### 3.1. AWP Mean

[5] In Figures 1a, 1b, and 1c, we show, respectively, the climatological JAS mean SST from EXPT-C, from observations [Reynolds *et al.*, 2002], and errors of EXPT-C. Unlike many of the IPCC AR4 models, the EXPT-C is able to simulate  $SST \geq 28.5^{\circ}C$  over the region. The AWP in the EXPT-C extends well into the GoM, the Caribbean Sea and the Atlantic Ocean. There is, however, widespread cold bias in EXPT-C (Figure 1c) over the AWP region with relatively large positive bias in the east Pacific Ocean. The

corresponding climatological mean JAS rainfall is overlaid in Figure 1. As mentioned earlier, in both the NCEP CFS and observations, rainfall is much higher in the surrounding land regions than over the AWP. The CFS has, however, some large positive bias in mean JAS rainfall over the eastern Pacific, the northwestern part of South America, and Central America. The seasonal cycle of the AWP SST variations are reasonably well captured by EXPT-C (Figure S2a of the auxiliary material). Furthermore, the seasonal variations of the heat flux in the EXPT-C (Figure S2b of the auxiliary material) are comparable to that in observations [cf. Wang and Enfield, 2001, Figure 2b]. By conducting heat budget analysis on an ocean general circulation model integration, Lee *et al.* [2007] conclude that clear sky radiation flux is the main driver for the seasonal onset and decay of the AWP. They further suggest that latent heat flux associated with reduced (increased) wind speed during the onset (decay) phase is consistent with a convective-evaporation feedback.

#### 3.2. Rain-SST Correlations

[6] Wu *et al.* [2006] succinctly described the merits of using rainfall-SST correlation in diagnosing the air-sea interaction in various regions of the tropics from forced and coupled ocean-atmosphere models. Positive SST anomalies can induce anomalous convection from destabilization of the atmosphere through enhanced surface evaporation and moisture flux convergence. This is indicated by positive local rainfall-SST correlation. On the other hand, atmospheric convection can feedback on SST from cloud-radiation, wind-evaporation effect and wind-induced oceanic mixing and upwelling [Wu *et al.*, 2006], which is usually reflected in negative rainfall-SST correlations. However, when monthly mean data is used (as it is here), the fast air-sea feedback cycles are unresolved and also affected by any existing atmospheric persistence. Therefore, it is suggested to examine lag-lead relationships [Cayan, 1992; Barsugli and Battisti, 1998; von Storch, 2000]. This is best accomplished by comparing the correlation of atmospheric fluxes with SST and the correlation of atmospheric fluxes with SST tendency [Wu and Kirtman, 2005; Wu *et al.*, 2006]. The simultaneous correlations of atmosphere fluxes-SST tendency could be interpreted as correlations across lag zero. For example, Wu *et al.* [2006] and Wu and Kirtman [2005] show that in regions where atmosphere forcing on SST is strong, the contemporaneous correlations of atmospheric flux with SST tendency is much larger than the simultaneous correlation of atmospheric flux with SST.

[7] In Figures 2a and 2b, we show the observed correlation between rainfall and SST and between rainfall and SST tendency respectively. The weak negative correlation over the GoM in Figure 2a simply suggests that the underlying SST does not force rainfall. Instead, the comparison of Figures 2a and 2b suggests that the atmospheric convection may be weakly forcing the SST evolution. The corresponding figures from EXPT-C in Figures 2c and 2d show that the SST in the NCEP CFS is probably responding to the atmospheric convection rather strongly, as depicted by the relatively large negative correlations in Figure 2d compared to that in Figure 2c over the Caribbean Sea and the northwestern tropical Atlantic Ocean. Similar bias of strong air-sea coupling in the NCEP CFS was also noticed

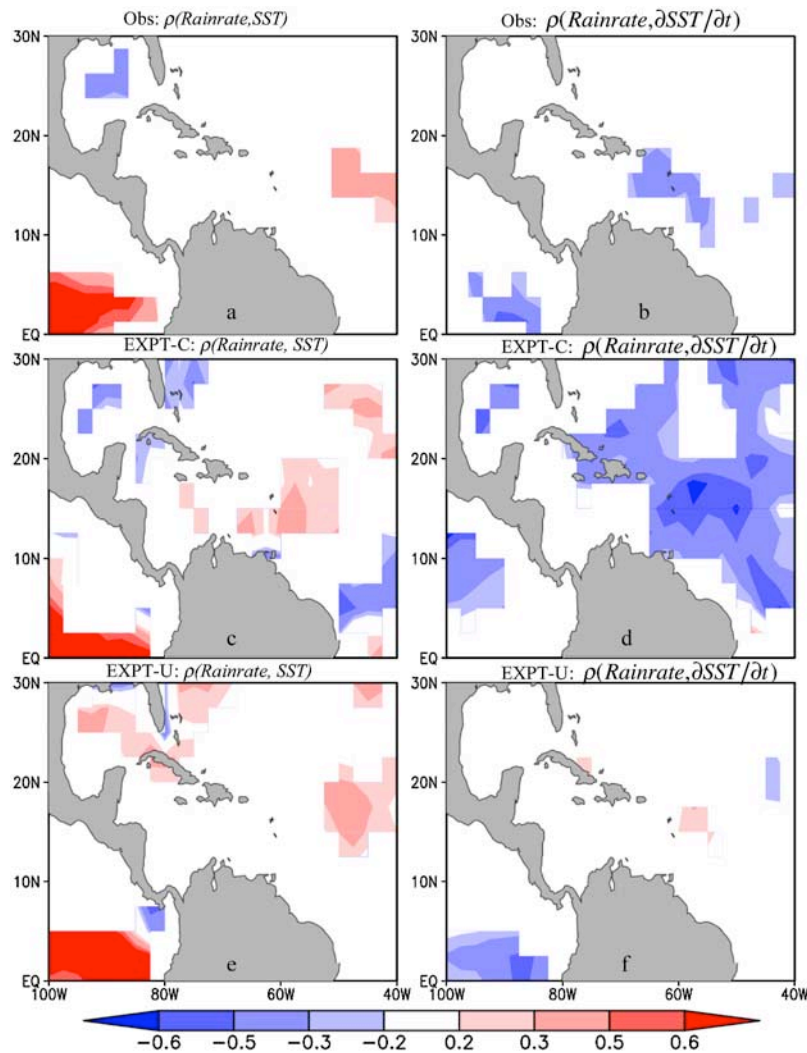


**Figure 2.** (a) Simultaneous correlation of rainfall and SST from observations (rainfall is from *Xie and Arkin* [1997] and SST is from *Reynolds et al.* [2002]). (b) Correlation of rainfall with SST tendency from observations. (c) Same as Figure 2a but from EXPT-C. (d) Same as Figure 2b but from EXPT-C. (e) Same as Figure 2a but from EXPT-U. (f) Same as Figure 2b but from EXPT-U. Only significant values at 90% confidence interval according to t-test are shaded.

over the tropical Indian Ocean [*Pegion and Kirtman*, 2008]. However, by design, the prescribed SST in EXPT-U is unable to respond to the atmospheric forcing. The simultaneous correlations of rainfall with SST in EXPT-U (Figure 2e) are positive over the GoM and the northwestern Atlantic Ocean with insignificant influence on SST tendency (Figure 2f). In other words, in EXPT-U the atmospheric convection is sensitive to the underlying SST anomalies, which is contrary to observations.

### 3.3. Relationship Between Latent Heat Flux and SST

[8] Surface evaporation is a dominant surface heat flux term in the tropical oceans and is directly related to air-sea feedback [*Zhang and McPhaden*, 1995; *Enfield*, 1996; *Chang et al.*, 1997; *Enfield and Lee*, 2005; *Wu et al.*, 2006]. The observed correlations of Latent Heat Flux (LHF) with SST and LHF with SST tendency are shown in Figures 3a and 3b, respectively. Here the observed fluxes are based on Goddard Satellite Based Surface Turbulence Fluxes [*Chou et al.*, 2003], available from July 1987 through December 2000). The fact that the simultaneous

correlations of LHF with SST tendency in Figure 3b are dominant over correlations between LHF and SST in Figure 3a suggests that SST variations are responding to LHF variations. This is similar to the Thermodynamic Air-sea Feedback (TAF) mechanism over the north tropical Atlantic Ocean [*Chang et al.*, 1997] as suggested earlier by *Enfield* [1996]. The TAF mechanism was originally proposed to explain the interhemispheric mode of tropical Atlantic SST variability. The TAF mechanism entails wind-induced changes in the turbulent heat flux and the modulation of the surface winds by the consequent developing meridional SST gradients. It may be noted that this result over the AWP is contrary to that of *Wang and Enfield* [2001], who claim that the TAF mechanism is weak over the AWP. In contrast, they showed that the cloud radiative feedbacks play a more prominent role over the AWP. This discrepancy between our study and that of *Wang and Enfield* [2001] may be highlighting the differences in the different sources of observational surface flux data used in the two studies. Furthermore, the lack of any significant simultaneous correlation between SST and rainfall over the

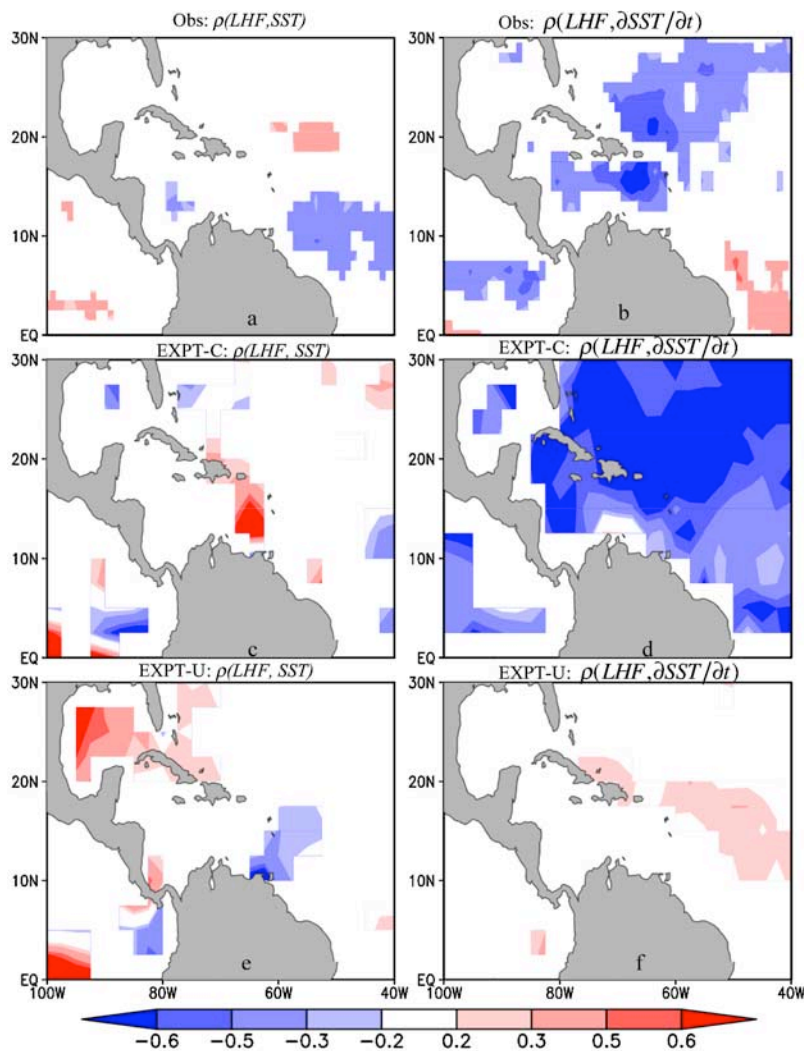


**Figure 3.** (a) Simultaneous correlation of latent heat flux and SST from observations (flux is from *Chou et al.* [2003] and SST is from *Reynolds et al.* [2002]). (b) The correlation of latent heat flux with SST tendency from observations. (c) Same as Figure 3a but from EXPT-C. (d) Same as Figure 3b but from EXPT-C. (e) Same as Figure 3a but from EXPT-U. (f) Same as Figure 3b but from EXPT-U. Only significant values at 90% confidence interval according to t-test are shaded.

AWP (Figure 2a) makes the cloud-radiative mechanism proposed by *Wang and Enfield* [2001] for the evolution of SST over AWP debatable. The large simultaneous negative correlation of LHF with SST tendency in EXPT-C (Figure 3d) compared to that with SST (Figure 3c) is qualitatively consistent with observations in Figures 3a and 3b. However, the strong negative correlations in Figure 3d over the western tropical Atlantic Ocean reflect the bias of the NCEP CFS to the SST being overly dependent on the LHF. EXPT-U shows a large positive correlation with SST over the GoM (Figure 3e) and, consistent with Figure 2f, shows insignificant correlations with SST tendency (Figure 3f). This once again points to the inadequacy of the forced AGCM integration in EXPT-U to resolve the air-sea interaction over the AWP.

### 3.4. Modulation of the Latent Heat Flux

[9] LHF can be modulated largely from surface winds and air-sea humidity differences. *Zhang and McPhaden* [1995] showed, in the context of the equatorial Pacific, that at seasonal time scales over very warm (moderate) SSTs, the

surface winds modulate LHF stronger (weaker) than the air-sea humidity difference. We have plotted similar correlations of LHF with air-sea humidity difference and wind speed in Figures 4a and 4b, respectively. Here, specific humidity at 10m and wind speed at 10m (obtained from the same dataset as *Chou et al.* [2003]) are used to compute air-sea humidity difference and wind speed respectively. The dependency of observed LHF on air-sea humidity and wind speed is comparable in magnitude, which is relatively weak and opposite in sign over the AWP. So the resulting observed LHF over the AWP is a subtle balance between the atmospheric dynamics (manifested by changes in surface wind speed) and local thermodynamics (manifesting as air-sea humidity difference). In EXPT-C, there is an over dependency of LHF on air-sea humidity difference (Figure 4c), while the influence of wind speed is comparably weaker and opposite in sign (Figure 4d). Similarly, EXPT-U shows the dominating influence of air-sea humidity difference on LHF (Figure 4e) with weaker influence of surface wind speed. The comparatively strong positive correlations between LHF and air-sea humidity difference found both

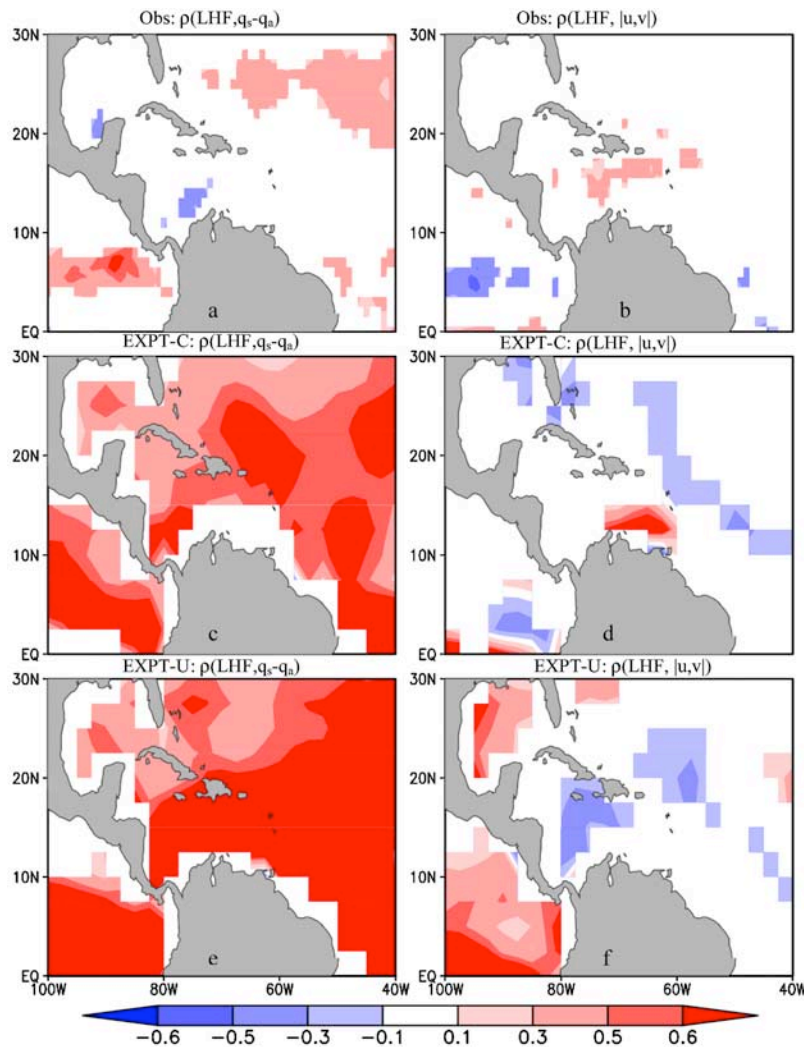


**Figure 4.** (a) Correlation of latent heat flux with air-sea humidity difference from observations (flux and air-sea humidity difference is from *Chou et al.* [2003]). (b) Correlation of latent heat flux with surface winds (at 10m) from observations (flux and winds are from *Chou et al.* [2003]). (c) Same as Figure 4a but from EXPT-C. (d) Same as Figure 4b but from EXPT-C. (e) Same as Figure 4a but EXPT-U. (f) Same as Figure 4b but from EXPT-U. Only significant values at 90% confidence interval according to t-test are shaded.

in EXPT-C and in EXPT-U suggest that this bias probably stems from the parameterization of the boundary layer scheme in the NCEP GFS, with the air-sea coupling damping this error to a certain extent in the NCEP CFS.

#### 4. Conclusions

[10] The absence of the AWP in many of the IPCC AR4 class of models is of grave concern, especially when it may have an influence on the boreal summer rainfall variations in the western hemisphere and the large-scale conditions that modulate Atlantic hurricane activity. In this study we have examined the air-sea interactions in the NCEP CFS integration and compared them with the NCEP GFS integration (where the AGCM is forced with observed SST). From observations and from this model inter-comparison, we find that the SST in the AWP responds to the atmospheric feedback. A case is therefore made that coupled ocean-atmosphere modeling is necessary to capture the evolution of the AWP, and forced AGCM integrations are

inadequate. However, errors in the parameterization scheme could exacerbate the errors in the coupled system as demonstrated in this study. The NCEP CFS suffers with a cold bias over the AWP region during the JAS season. It is shown that coupled air-sea feedback in the NCEP CFS is significantly stronger than observations, especially over the northwestern tropical Atlantic Ocean. This seems to stem from the strong modulation of air-sea humidity variations on the LHF in both the NCEP CFS and the NCEP GFS.

[11] **Acknowledgments.** I would like to acknowledge the expert guidance of Meredith Field of COAPS for her editorial corrections on an earlier version of the manuscript. This research was supported by NOAA grant NA07OAR4310221.

#### References

- Barsugli, J. J., and D. S. Battisti (1998), The basic effects of atmosphere-ocean thermal coupling on midlatitude variability, *J. Atmos. Sci.*, *55*, 477–493, doi:10.1175/1520-0469(1998)055<0477:TBEAOA>2.0.CO;2.
- Cayan, D. R. (1992), Latent and sensible heat flux anomalies over the northern oceans: Driving the sea surface temperature, *J. Phys. Oceanogr.*, *22*, 859–881, doi:10.1175/1520-0485(1992)022<0859:LASHFA>2.0.CO;2.

- Chang, P., L. Ji, and H. Li (1997), A decadal climate variation in the tropical Atlantic Ocean from thermodynamic air-sea interactions, *Nature*, 385, 516–518, doi:10.1038/385516a0.
- Chou, S.-H., E. Nelkin, J. Ardizzone, R. M. Atlas, and C.-L. Shie (2003), Surface turbulent heat and momentum fluxes over global oceans based on Goddard satellite retrievals, version 2 (GSSTF2), *J. Clim.*, 16, 3256–3273, doi:10.1175/1520-0442(2003)016<3256:STHAMF>2.0.CO;2.
- Enfield, D. B. (1996), Relationships of inter-American rainfall to tropical Atlantic and Pacific SST variability, *Geophys. Res. Lett.*, 23, 3305–3308, doi:10.1029/96GL03231.
- Enfield, D. B., and S.-K. Lee (2005), The heat balance of the western hemisphere warm pool, *J. Clim.*, 18, 2662–2681, doi:10.1175/JCLI3427.1.
- Lee, S.-K., D. B. Enfield, and C. Wang (2007), What drives the seasonal onset and decay of the western hemisphere warm pool?, *J. Clim.*, 20, 2133–2146, doi:10.1175/JCLI4113.1.
- Pegion, K., and B. P. Kirtman (2008), The impact of air-sea interactions on the simulation of the tropical intraseasonal variability, *J. Clim.*, 21, 6616–6635, doi:10.1175/2008JCLI2180.1.
- Reynolds, R. W., N. A. Rayner, T. M. Smith, D. C. Stokes, and W. Wang (2002), An improved in situ and satellite SST analysis for climate, *J. Clim.*, 15, 1609–1625, doi:10.1175/1520-0442(2002)015<1609:AIISAS>2.0.CO;2.
- Ruiz-Barradas, A., and S. Nigam (2005), Warm season rainfall variability over the U. S. Great Plains in observations, NCEP and ERA-40 reanalyses, and NCAR and NASA atmospheric model simulations, *J. Clim.*, 18, 1808–1830, doi:10.1175/JCLI3343.1.
- Saha, S., et al. (2006), The climate forecast system at NCEP, *J. Clim.*, 19, 3483–3517, doi:10.1175/JCLI3812.1.
- von Storch, J.-S. (2000), Signature of air-sea interactions in a coupled atmosphere-ocean GCM, *J. Clim.*, 13, 3361–3379, doi:10.1175/1520-0442(2000)013<3361:SOASII>2.0.CO;2.
- Wang, C., and D. B. Enfield (2001), The tropical western hemisphere warm pool, *Geophys. Res. Lett.*, 28, 1635–1638.
- Wang, C., and D. B. Enfield (2003), A further study of the tropical western hemisphere warm pool, *J. Clim.*, 16, 1476–1493.
- Wang, C., D. B. Enfield, S.-K. Lee, and C. W. Landsea (2006), Influences of the Atlantic warm pool on western hemisphere summer rainfall and Atlantic hurricanes, *J. Clim.*, 19, 3011–3028, doi:10.1175/JCLI3770.1.
- Wang, C., S.-K. Lee, and D. B. Enfield (2008a), Climate response to anomalously large and small Atlantic warm pools during the summer, *J. Clim.*, 21, 2437–2450, doi:10.1175/2007JCLI2029.1.
- Wang, C., S.-K. Lee, and D. B. Enfield (2008b), Atlantic Warm Pool acting as a link between Atlantic Multidecadal Oscillation and Atlantic tropical cyclone activity, *Geochem. Geophys. Geosyst.*, 9, Q05V03, doi:10.1029/2007GC001809.
- Wu, R., and B. P. Kirtman (2005), Roles of Indian and Pacific Ocean air-sea coupling in tropical atmospheric variability, *Clim. Dyn.*, 25, 155–170, doi:10.1007/s00382-005-0003-x.
- Wu, R., B. P. Kirtman, and K. Pegion (2006), Local air-sea relationship in observations and model simulations, *J. Clim.*, 19, 4914–4932, doi:10.1175/JCLI3904.1.
- Xie, P., and P. A. Arkin (1997), Global precipitation: A 17-year monthly analysis based on gauge observations, satellite estimates, and numerical model outputs, *Bull. Am. Meteorol. Soc.*, 78, 2539–2558, doi:10.1175/1520-0477(1997)078<2539:GPAYMA>2.0.CO;2.
- Zhang, G. J., and M. J. McPhaden (1995), The relationship between sea surface temperature and latent heat flux in the equatorial Pacific, *J. Clim.*, 8, 589–605, doi:10.1175/1520-0442(1995)008<0589:TRBSST>2.0.CO;2.

---

S. Chan and E. Chassignet, Center for Ocean-Atmospheric Prediction Studies, Florida State University, Tallahassee, FL 32306, USA.

V. Misra, Department of Meteorology, Florida State University, Tallahassee, FL 32306, USA. (vmisra@fsu.edu)

R. Wu, Center for Ocean-Land-Atmosphere Studies, 4041 Powder Mill Road, Suite 302, Calverton, MD 20705, USA.

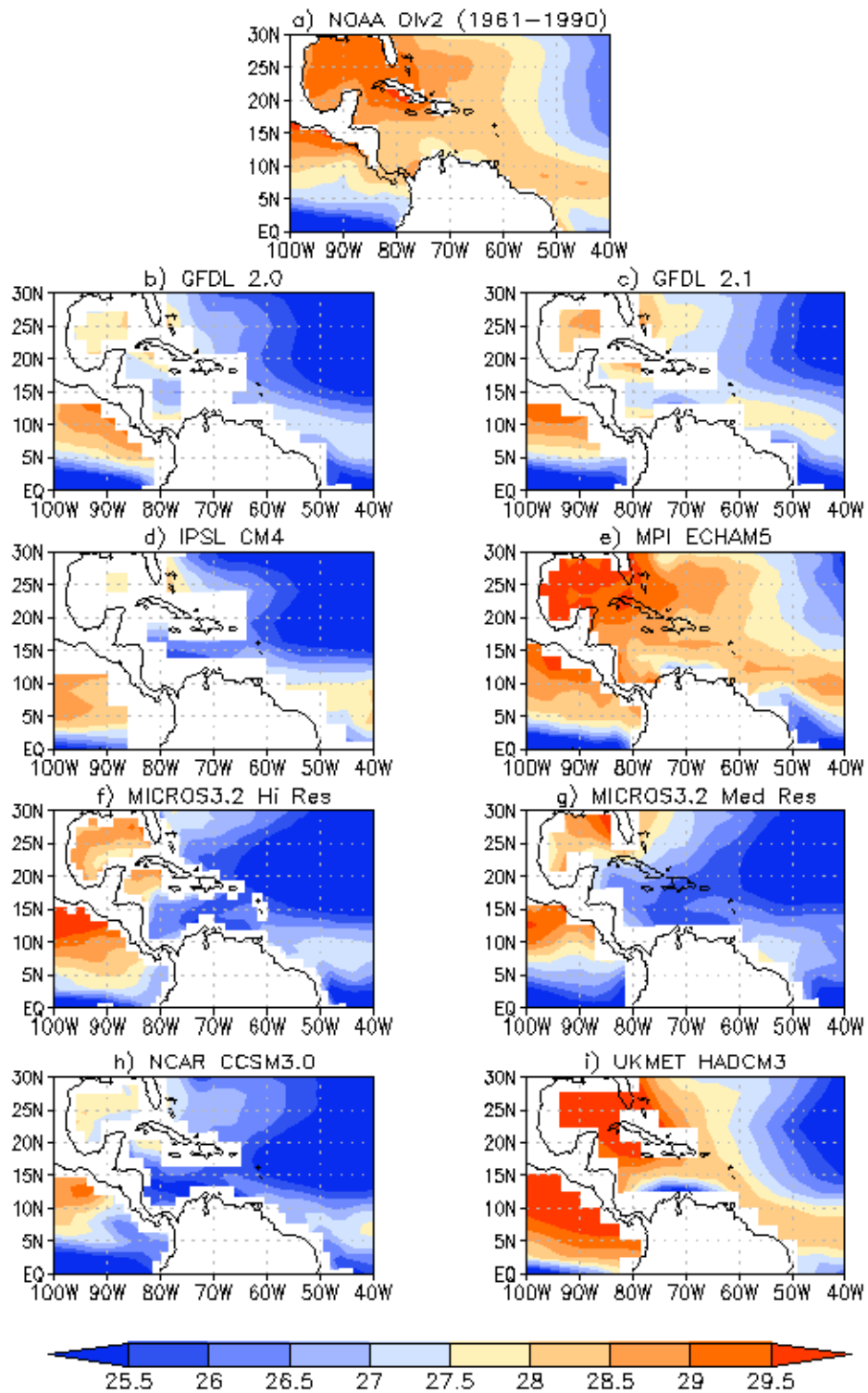


Figure 1: The July-August-September (JAS) climatological mean SST from a) Observations and b, c, d, e, f, g, h, i) eight IPCC –AR4 models.

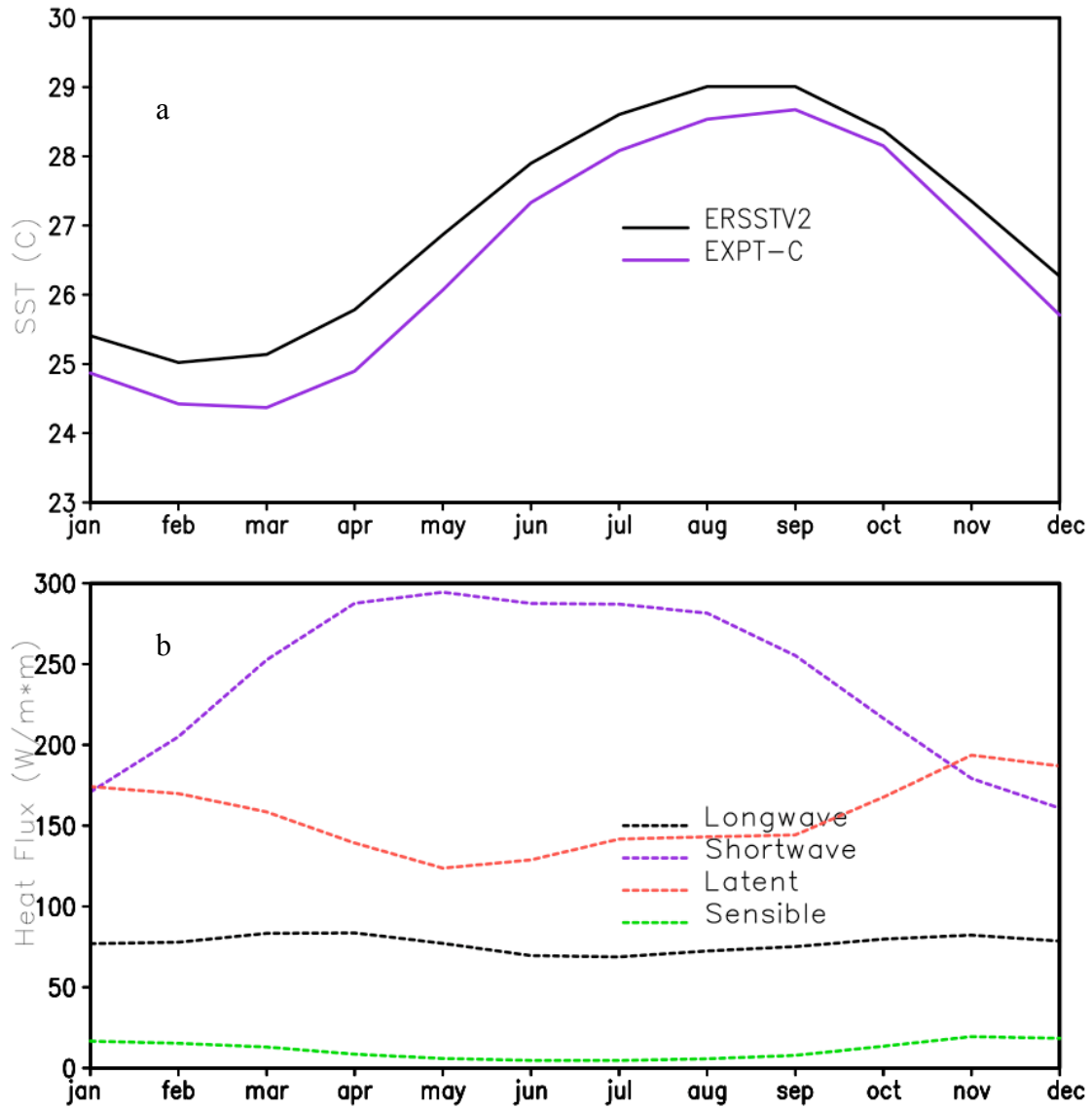


Figure 2: (a) Seasonal variations of SST over the Atlantic warm pool ( $95^{\circ}W-65^{\circ}W$ ,  $13^{\circ}N-30^{\circ}N$ ). (b) Seasonal variations of the longwave, shortwave, latent and sensible heat flux averaged over the AWP region from the EXPT-C integration.